System Modelling of Alveolar Epithelial Tissue and the Effects of Particulate Matter on Human Health using COBWEB

Liam Foyle
ENV299
Research Director: Professor Brad Bass
April 12th, 2020

Introduction

Particulate Matter (PM) and its effect on human health is an important field of study that needs to be undertaken to ensure the health and safety of the world's population. PM has serious health effects, including exacerbating preexisting conditions, causing heart and lung disease, respiratory inflammation, and even premature death[2-10].

COBWEB, *Complexity and Organized Behaviour Within Environmental Bounds*, is a computer modeling system that is able to address the research of a multitude of topics. COBWEB was used to model alveolar epithelial tissue, and the effect that PM has on the generation of Reactive Oxygen Species (ROS) through Fenton type reactions with iron and Polycyclic Aromatic Hydrocarbons (PAH).

The model answers the questions: *what is the synergistic relationship between iron and PAH within human alveolar tissue and how does it compare to other studies? Moreover, on the cellular level, is it possible to see a relationship between tissue destruction and ROS concentration/reactivity?* It provides an in-depth look into the structure and operation of human lung tissue.

Literature Review

Introduction

Environment and Climate Change Canada (ECCC) is the regulatory body tasked with protecting and preserving Canada's natural and urban environments. Included in their mandate is the protection of Canadian citizens from harmful or toxic substances in the environment which includes ensuring clean and breathable air[1]. One of the key pollutants regulated is Particulate Matter (PM)[1]. The human health implications and its research will be thoroughly discussed in this review.

PM as defined by the ECCC "consists of airborne particles in the solid or liquid phase" [2]. Baird and Cann[3] define PM as "tiny solid or liquid particles - other than those of pure water - that are temporarily suspended in air, and that are usually invisible to the naked eye." Colloquially, various terms are used, including mist or fog for liquid particulates, and dust or soot for solid particulates[3]. Throughout human history, air pollutants and PM have enveloped cities and caused severe health implications: London in 1952 from homes burning coal, killing several thousand; Los Angeles in the 40s and the orange haze, also known as photochemical smog, scattered over the city from car pollution; Beijing in the 90s with thick blankets of PM covering the city and restricting visibility[4].

Formation, Composition, and Classification

To fully understand how PM affects human health, it is important to understand the main concepts behind PM: formation, composition, and classification. The formation and composition of PM is quite complicated, as there are regional and geographic implications [4,5]. The majority of these factors comprise sources of pollution in the vicinity, the topography (especially peaks and valleys), and meteorology (wind patterns)[4].

Environmental chemists classify 2 types of pollutants: primary, and secondary[3]. Primary pollutants are substances directly released from sources that can affect the environment, while secondary pollutants are formed from the decomposition or other various reactions of primary pollutants[3]. These pollutants include: organic carbon (alkanes, alkenes, aldehydes, aliphatic hydrocarbons, and Polycyclic Aromatic Hydrocarbons (PAHs)), black carbon, sulfate, nitrate, ammonium, trace metals (magnesium, copper, zinc, chromium, and selenium), as well as, heavy metals including lead, mercury, and arsenic, and all of their derivatives after reaction in the troposphere[3-7]. All of these pollutants come from a variety of sources, but transportation and

energy production are some of the largest[4,6]. These emitted pollutants undergo processes called nucleation and surface growth to form PM[7]. Nucleation occurs when small gas molecules condense with molecules in the solid or liquid phase, combining to form very small PM, while surface growth occurs when molecules or particles add on to existing, nucleated PM[7].

PM can then be classified into two fundamental size ranges: coarse and fine, where coarse represents particles with a diameter larger than 2.5 µm, and fine less than this[3]. However, in environmental regulation, the definition changes slightly: although PM extends to between 100 µm and 0.002 µm, PM_{10} and $PM_{2.5}$ are the main particulates regulated, where PM_{10} has a diameter less than 10 µm, and $PM_{2.5}$ has a diameter less than 2.5 µm[2,3]. Ultrafine PM is classified as having a diameter less than 0.1 µm, but are under intense research as little is known about their deleterious effects[8].

Health Effects Introduction

It has been well documented in scientific literature that the size of PM is directly linked to the deleterious effects: as PM gets smaller, it gets more dangerous to human health[3,4,7-10]. Moreover, scientists believe there is no safe level of PM in the troposphere[10]. PM is linked to various adverse health effects ranging from exacerbating pre existing allergies, causing heart and lung disease, triggering respiratory inflammation, to premature death[2-10]. To understand the health effects, the method of entry must first be established, and then deposition and distribution of PM throughout the body needs to be explored.

Methods of Entry, Deposition, and Distribution

PM has two known methods of entering the body: inhalation, and ingestion[10]. Absorption through the skin and through medical injections are still under review and research[10]. With ingestion, PM being swallowed through food consumption is one method, while the ingestion of

mucus through the mucociliary transport is the main method[10]. This is because PM greater than 10 µm in diameter get trapped by the cilia and mucus in human's nasal passage[8]. After settling in the throat or upper bronchial passages, this PM can be expelled through processes like sneezing and coughing, where the PM can then be ingested [8,10]. This new field of research is then determining how PM influences chronic diseases like Crohn's and inflammatory bowel, appendicitis, and cancer in the gastrointestinal tract[10].

Inhalation is the route wherein PM is breathed in through the three regions of the human airway system: the head airways (which include the nose, mouth, pharynx, and larynx), the tracheobronchial region, and the alveolar region[10]. New studies suggest that PM between 5 and 10 µm are generally deposited in the tracheobronchial tree, while PM between 1 and 5 µm are deposited in the respiratory bronchioles, where they can then enter into the bloodstream and affect a multitude of systems, including the gastrointestinal, reproductive, cardiovascular, and pulmonary system[4].

However, other newer studies suggest that PM greater than 1 µm, or less than 0.01 µm are deposited in the head airways, while PM less than 1 µm and greater than 0.02 µm represent the greatest threat to deposition within pulmonary tissue[10]. This is due to the fact that the PM greater than 1 µm deposit on to airways, and are effectively removed by mucociliary processes, while PM less than 0.01 µm easily diffuse in the head airways, as the PM is so small, it is effectively acting as a gas[10]. This is not to say that these sizes of PM are still not deleterious to other regions of the body, as ultrafine PM diffused in the head airways are able to deposit on the olfactory nerve, and eventually reach the brain[10].

In one study, PM was seen throughout the pulmonary artery, the peribronchial tissues, and the adjacent alveolar septal walls in previously deceased males in California[9]. This is a key finding, as these structures in and around the bronchioles have highly specialized cells, including ciliated cells, nonciliated bronchiolar epithelial cells, and neuroendocrine cells, that take damage with high uptake of PM[9].

The body has methods for removal of PM from deposition within pulmonary tissue, which include macrophage phagocytosis, PM transport to lung lymph nodes, and dissolution into the blood[10]. Macrophage phagocytosis is very effective at removing PM, but this results in inflammation, as inflammation occurs from cytokines being released, mediated by highly active macrophages, neutrophils, and epithelial cells [8,10].

Reactive Oxygen Species Formation

One of the major contributors to producing highly active macrophages, neutrophils, and epithelial cells from the deposition of PM is the oxidative stress placed on the pulmonary tissue[10-14]. This oxidative stress is created by an excess of Reactive Oxygen Species (ROS), when the bodies natural antioxidants are overwhelmed [11-14]. This is due to the indiscriminate redox chemistry of ROS - when there are no antioxidants, they chemically change DNA, proteins, lipids, cause cell and tissue damage, and even cellular apoptosis[12]. Some of these ROS include free radicals, which are extremely reactive species having one unpaired electron, like the hydroxyl (·OH), hydroperoxy (·OOH), alkoxy (·OR), alkylperoxy radicals (ROO·), and reactive species including superoxide radical anion (O_2^-), hydrogen peroxide (H_2O_2), and ozone (O_3)[10,12].

PM can either contain these reactive species, or, they have the precursors within them that end up creating these harmful species within the pulmonary cells and tissue[12]. Some of the major contributors to the production of these ROS are transition metals, and in particular,

iron[8,10,13,14]. Iron is necessary for human life, but not in pulmonary tissue - when iron is deposited, it undergoes the Fenton reaction, with the mechanism shown below [8,10,11-13,15].

$Fe^{2+} + H_2O_2 \rightarrow Fe^{3+} + \cdot OH + OH^-$

Where the radical species ·OH is formed (hydroxyl radical). Fe^{3+} can then react with other ROS to form Fe^{2+}, forming a catalytic cycle.

This catalytic cycle is quite detrimental, as the reformation of Fe^{2+} allows for the continuing generation of ROS, adversely affecting pulmonary tissue. Moreover, it becomes more complicated with the implications of Polycyclic Aromatic Hydrocarbons (PAHs), and quinones within PM, as a synergistic effect has been shown between iron, PAHs, and quinones[10,13]. The quinones can form hydrogen peroxide, which can then be catalytically broken down into ROS by iron[13].

Physiology of Alveolar Epithelial Tissue

Lastly, after a basic understanding of the chemistry behind formation of ROS and deposition of PM is formed, a basic understanding of alveolar epithelial tissue can be developed.

Alveolar epithelial tissue is a continuous lining of epithelial cells within the lung[16]. These epithelial cells, also called pneumocytes, are the most abundant cells in the lung and can be broken into two classes: Type I and Type II[16,17]. Type I pneumocytes cover a larger area of the alveolar tissue, as these are the simplest cells within the lung that allow for gas exchange[16]. Type I cells are long and thin, with a small nucleus[16]. Type II cells are bulkier, more cubic in shape, and not as prevalent within alveolar tissue as they do not regulate gas exchange[16]. Their function is production of surfactant, which is critical for gas exchange, as it lowers the surface tension of the interstitial fluid, allowing for gas molecules to diffuse in high concentrations[16].

These cells form a mesh network with capillaries within the alveoli, while the space in between the cells is called the alveolar interstitial space. Figure 1 depicts the cellular structure.

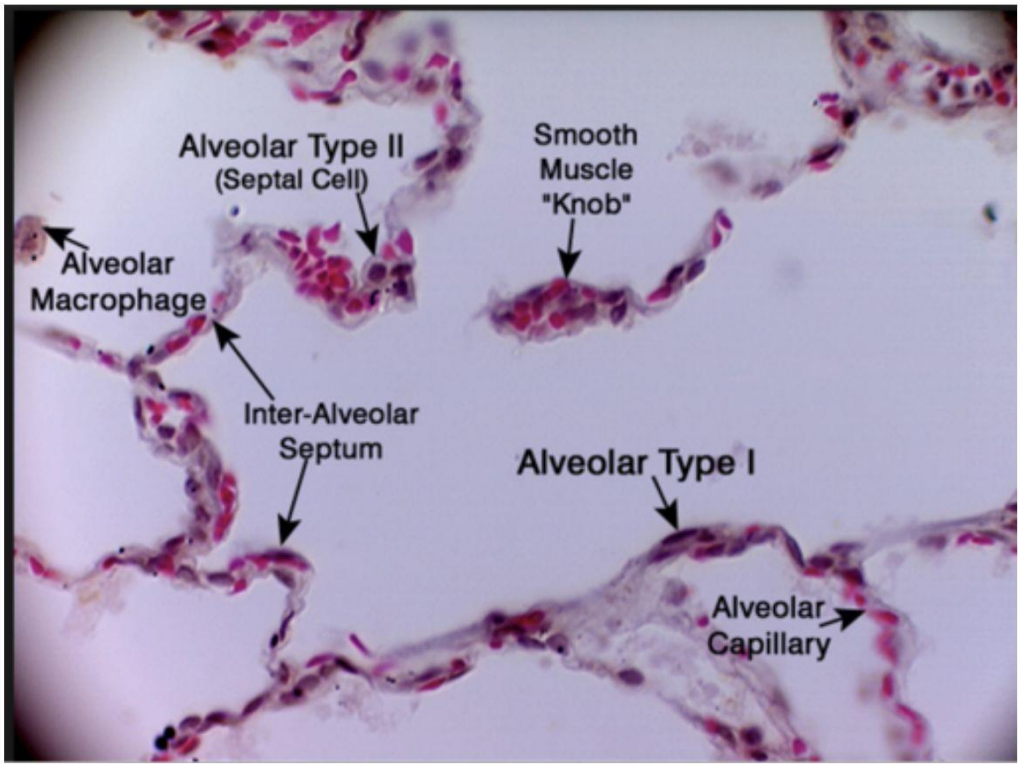

Figure 1: Courtesy of ANA300 at the University of Toronto, depicting Type I & Type II cells; interstitial space is representative of the white background

Moreover, alveolar macrophages are the main removal and transport of fine particulate matter, while also helping contribute and signal the immune response to foreign particles[16].

Conclusion

It is quite well documented that the study of PM, whether it is in the formation and composition, the distribution throughout the body, or the health effects presented from these varying particles is quite complicated.

Mice have been the main source of studies in measuring the health effects of PM, as it is not ethical to do *in vivo* studies on humans. A study looking at the possible roles of metals in

inflammatory and defence responses was recently completed in 2015[14]. Here, mice were subject to the inhalation of collected roadside particulate matter, specifically containing various metals[14]. Their immune responses were measured 24 and 48h later[14]. Specifically, the researchers were looking at the amount of metals and PM-induced inflammation in lung tissue, by studying the Broncho-Alveolar Lavage Fluid (BALF)[14].

A varying amount of immune response mechanisms including NF-E2-related factor-2 (NrF2), interleukin-6 (IL-6), and Tumor Necrosis Factor alpha (TNF-α), all cytokines (proteins that induce the inflammation of tissue), were all measured to be higher after oxidative stress was induced from PM after 24 hours, but not after 48 hours[14].

Moreover, other research has focused on the concentration of ROS in Epithelial Lining Fluid (ELF) in humans, using a system called Kinetic Multi-Layer Model of Surface and Bulk Chemistry in the Epithelial Lining Fluid[18]. This is to address the major lack of research done in the area of kinetics of ROS within the respiratory system. The study found that as $PM_{2.5}$ increases logarithmically from 1 μg/m^3 to 1000 μg/m^3, ROS also increases logarithmically, but not on the same order of magnitude, ranging from 1 nmol/L to 250 nmol/L[18]. Although the kinetics behind the Fenton type reactions within the body are quite complex and are difficult to model, they are vital to the formation of ROS, where iron is the most efficient catalyst for hydroxyl production[18].

It is between these studies and the use of COBWEB that the questions can be posed: *what is the synergistic relationship between iron and PAH within human alveolar tissue and how does it compare to other studies? Moreover, on the cellular level, is it possible to see a relationship between tissue destruction and ROS concentration/reactivity?*

Methods

To address these research questions in an ethical manner in which both human and animal life are not exposed to the risks of particulate matter, system modelling can be a very valuable tool. Moreover, system modelling allows for a deeper look at cellular processes, which in the laboratory, would not be possible with the same accessibility or ease.

COBWEB is a computer modelling tool created to address real world systems revolving around the ideology of complexity.

Within the system, *agents* (represented by triangles) are able to move and consume food; they can reproduce, eat one another, be restricted in area and movement, and produce waste. Their food source (represented by squares) can grow and spawn, and also be restricted by area. The complexity of the system lies within the random genetic algorithms that tell the agents how to react and move; moreover, the interconnectedness of the agents gives the simulation a real-world applicability, where an agent or collective agents' decisions can have major impacts on other agents, as well as the system as a whole.

In modelling alveolar epithelial tissue within COBWEB, there are different options in presentation; a more visual model replicating the structure or a more empirical approach where agent populations represent different cellular processes. In this paper, a combination of the two was taken to obtain a full scope of the synergistic effect between iron and PAH in relation to production of ROS, as well as how ROS degrades cellular membranes.

The island parameter within the agent abiotic tab, which restricts the movement of agents, was used to create two cell membrane like structures, by placing a smaller island within a larger island. This forced agents 1 and 2 into oval and cubic like shapes, respectively, representing both type I and type II pneumocyte cell membranes. Agents 1 and 2 are designed to

represent the mosaic of moving phospholipids and other proteins within the cell membrane. The island parameter was also used to form nucleic structures by placing islands within the cell. This is where agents 4 and 5 would reside, representing the genetic material present in both pneumocytes.

Two angled split parameters from the agent abiotic tab were also set up at an angle of 14 degrees, and set at the top of the model where agent 3 was used to represent the capillary mesh present in alveolar epithelial tissue.

The interstitial space was set using the split parameter from the agent abiotic tab, where agents 6 and 7 were confined, representing the process of deposition of fine and ultrafine particles within the alveolar epithelial tissue. Agents 6 and 7 were then able to mate, under COBWEB's new mating functionality, to produce agent 8. This represents the reaction between iron and PAH to produce ROS. This catalytic cycle is quite complicated, as various products including hydroxide ($\cdot OH$) and superoxide (O_2^-) radicals react with other PAH and organic molecules that may not have been reactive or detrimental to human health, and turn them into reactive species[10,12]. This propagates radical formation. For this model, a simplified agent 6 +7 to form 8 was used to model the creation and reaction of ROS within the cells.. Figure 2 depicts the model before any experiments were completed.

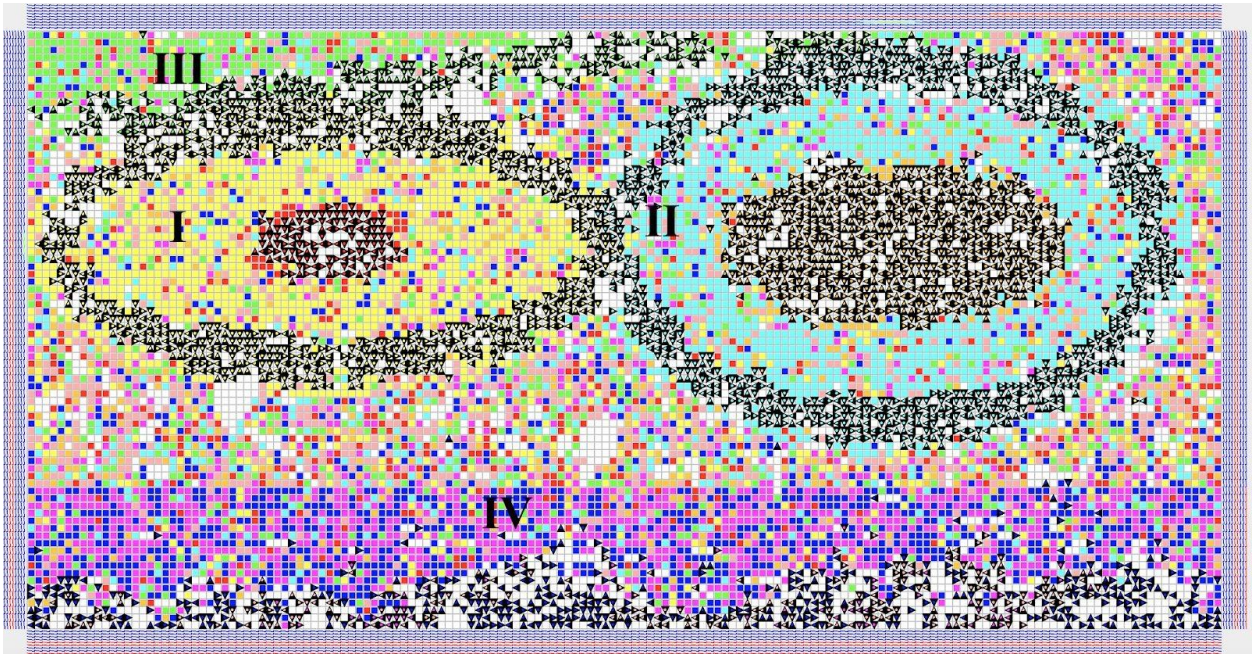

Figure 2: Agents are triangles, and their food is the coloured squares; I and II represents type I and II pneumocytes, respectively; III represents the capillary mesh interconnected with the pneumocytes (green agents); IV represents the interstitial space, the blue and pink agents represent iron and PAH, while the third agent coloured light pink is formed completely from the mating of the blue and pink agents.

Before the experiments were run, it is important to note that the cell structures (both cell membranes, the nuclei, and the capillary mesh) were artificially introduced into the model. This was done by selecting the *Edit* pull down tab, and clicking on the respective agent in *select agents.* The agents were then placed in the areas where they were expected to form, to speed up the time of experiments. This is depicted in figure 3.

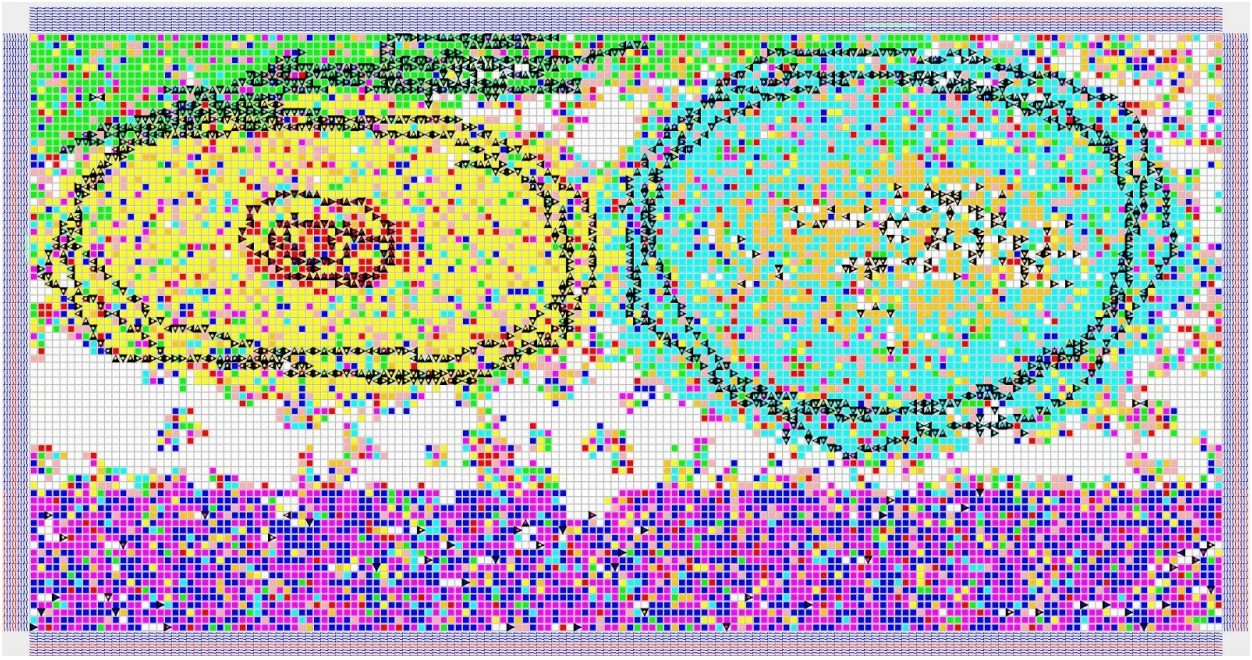

Figure 3: Artificial Production of cell membranes as well as nuclei and mesh network of capillaries through placement of agents. Figure 3 is the starting point of the organization of the system through agent manipulation.

10 experiments were run in total, each containing two parts to each experiment. For the first part of the experiment, the independent variable was the mating chance between agents 6 and 7, while the dependent variable was the population of agent 8. This is the representation of the effective reactivity of the iron and PAH in solution; an increase of the mating parameter represents more chemical potential in the system. Note, the independent variable was not the initial populations of agents 6 or 7, rather just their ability to mate. This can be viewed from a chemical viewpoint as having reactive species in solution that can create greater amounts of ROS due to their reactivity, not to a change in their initial concentrations. The model was run until 500 ticks, at which point the population of agent 8 was recorded.

Next, due to the nature of the model, agent 8 was not able to move effectively towards the cells. At this point, the model was paused, the population of agent 8 formed in the interstitial space, and moved towards the cells. The model was then restarted, and ran until 750 ticks.

In the second part of the experiment, the independent variable was the population of agent 8, with the dependent variables being the change in the population of agents 1 and 2. This represents how the degradation of the cell membranes change with the increase of ROS.

The data was inputted into an Excel spreadsheet, plotted and curve fitted, and the relationships between the independent and dependent variables was determined.

Results

The results are shown below in tabular, and visual form through tables 1 through 3, and figures 4 through 10. The first segment of the experiment is shown below:

Mating Parameter Probability	Population of Agent 8
0.1	79
0.3	201
0.5	175
0.75	371
1	286
1.5	410
2	291
3.5	304
5	212
10	373

Table 1: Mating Parameter Probability vs Population of agent 8, not averaged

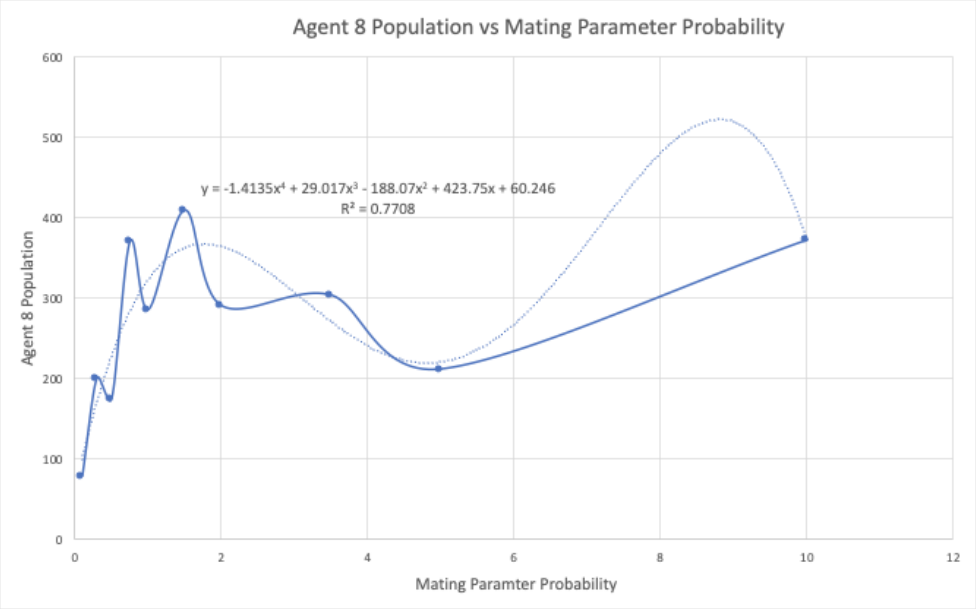

Figure 4: Graph of agent 8 population vs mating parameter probability, not averaged, with a curve fit performed

There is a large amount of noise within the data set. Moreover, the quartic function fit does not fit well with the curve. The poor correlation coefficient of 0.77 represents a large margin of error, and the large concave down portion on the right side of the plot does not follow the data. Therefore, a pairwise average was formed for the points to eliminate as much noise as possible, with the first and last point unmodified, resulting in table 2 and figure 4.

Mating Parameter Probability	Population of Agent 8
0.1	79
0.4	188
0.625	272
0.875	328.5
1.25	248
1.75	350.5
2.75	297.5
4.25	258
7.5	292.5
10	373

Table 2: Pairwise average of mating parameter probability and population of agent 8

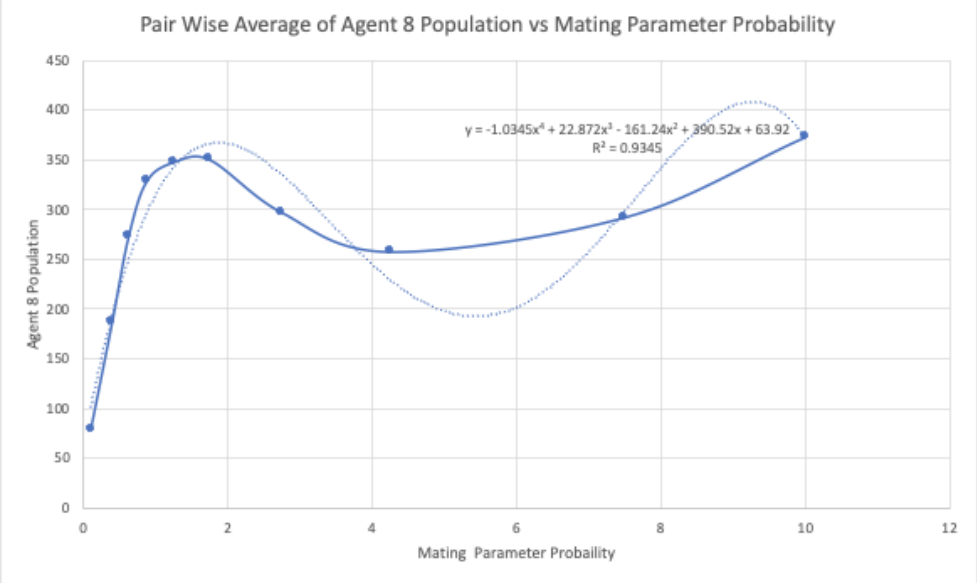

Figure 5: Pairwise Average of Agent 8 Population vs Mating Parameter Probability, Eliminating the noise

These tables and figures represent the first segment of the experiment: determining the relationship between ROS production and the reactivity of PM present within the lung tissue. It

is shown the relationship from the pairwise average of Agent 8 population vs Mating Chance Parameter is of the form:

$$y = -1.034\,x^4 + 22.872\,x^3 - 161.24\,x^2 + 390.52\,x + 63.92$$

The results for the second segment of the experiments are shown below:

Agent 8 Population	**ΔPopulation of Agent 1 Between Ticks 500 and 750**	**ΔPopulation of Agent 2 Between Ticks 500 and 750**	**Total Loss of Agents 1 and 2**
79	24	65	89
201	81	8	89
175	38	45	83
371	-2	32	30
286	36	12	48
410	34	50	84
291	8	3	11
304	53	55	108
212	38	5	43
373	28	24	52

Table 3: Cumulative Data of Second Segment of Experiment 2, where delta represents initial minus final

To present in a clear manner, figures 6, 7, and 8 are separated from one another:

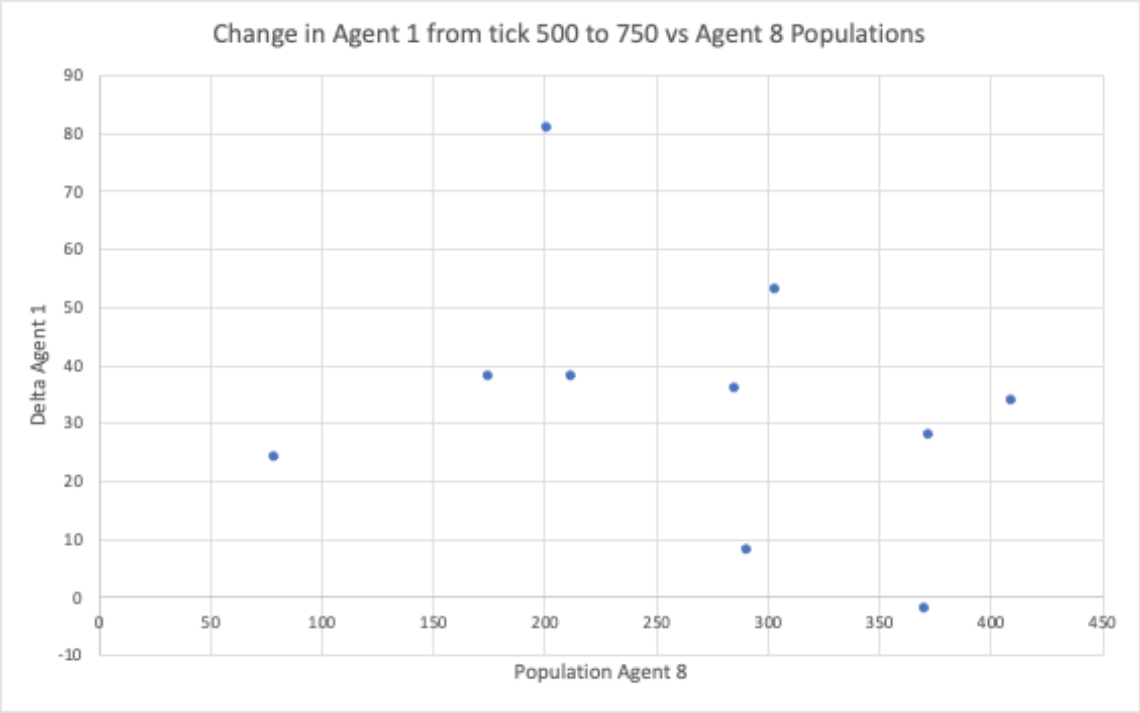

Figure 6: Representation of 250 tick time span for change in Agent 1 Population vs Agent 8 Population

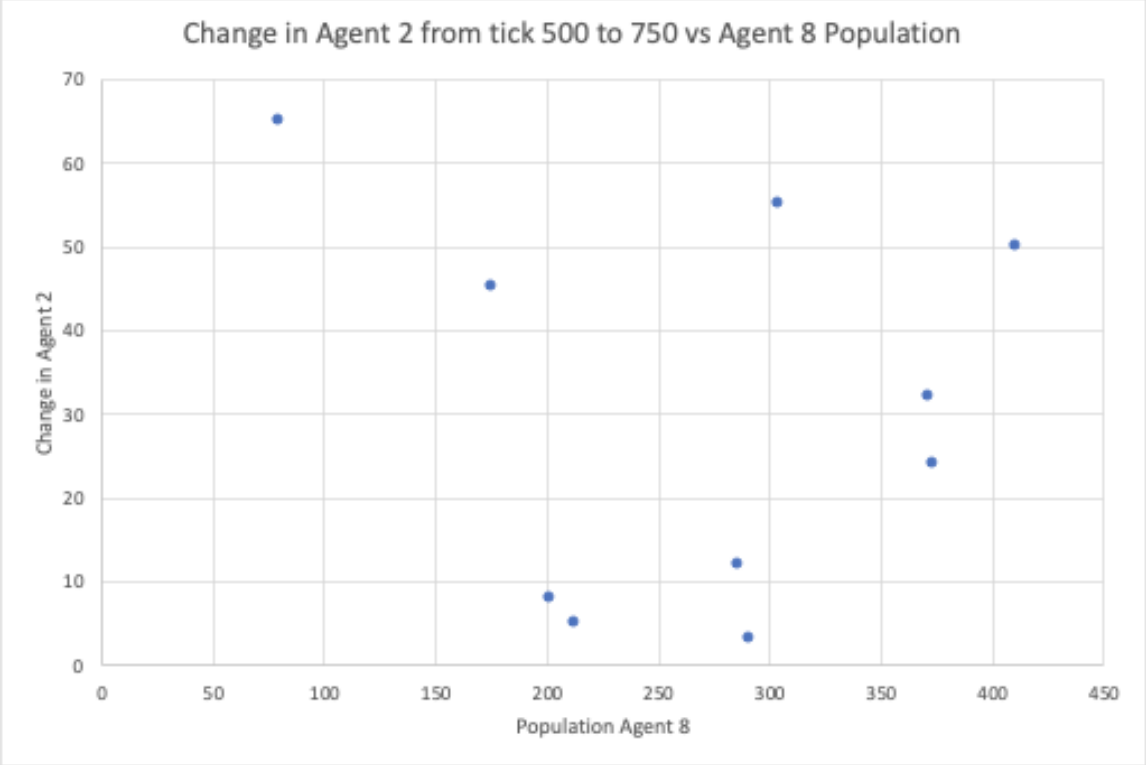

Figure 7: Representation of 250 tick time span for change in Agent 2 Population vs Agent 8 Population

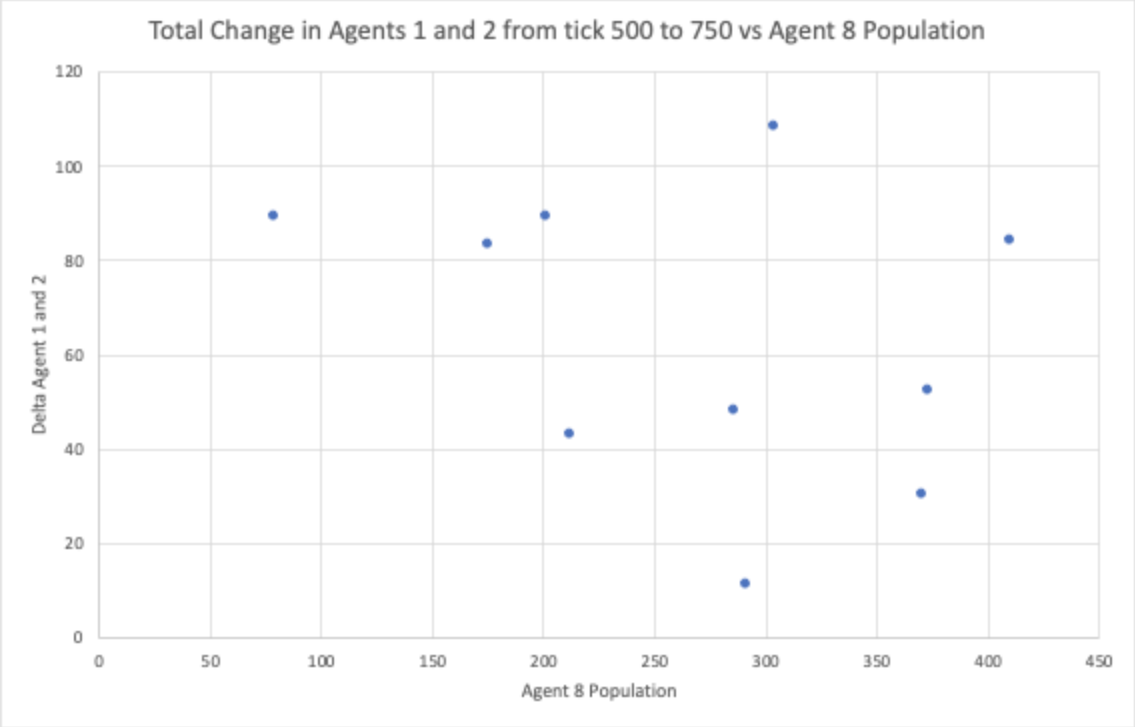

Figure 8: Representation of 250 tick time span for total change in Agent 1 and 2 population vs Agent 8 Population

A visual representation of the results is shown in figures 9 and 10.

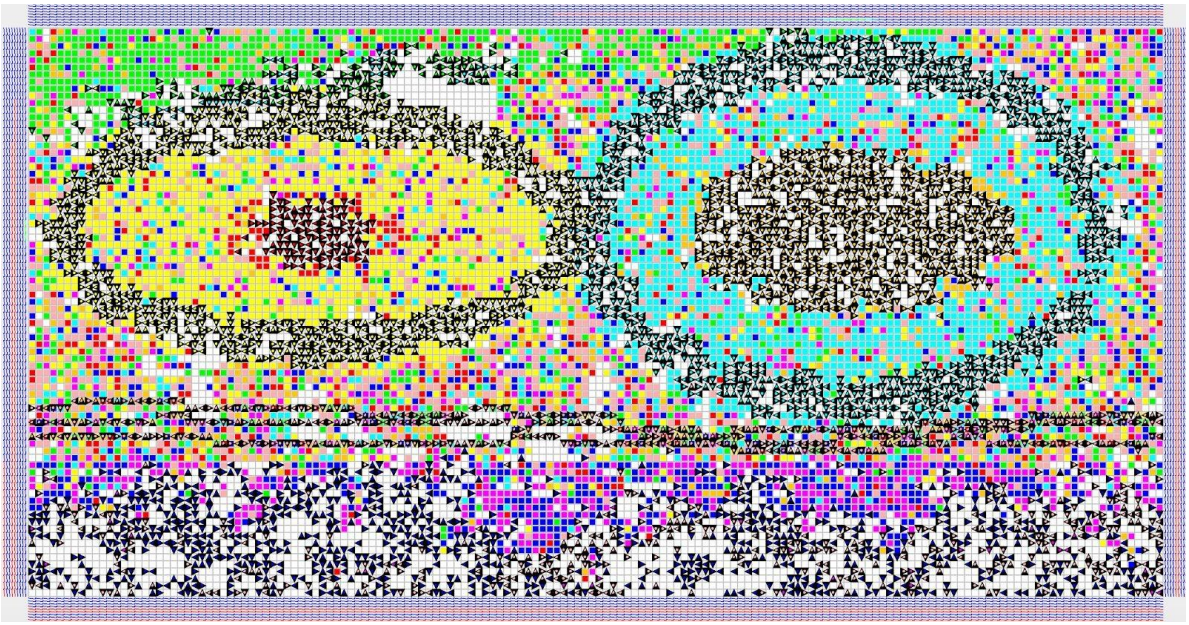

Figure 9: Population of Agent 8 (ROS) is tabulated and moved from the interstitial space towards the cells

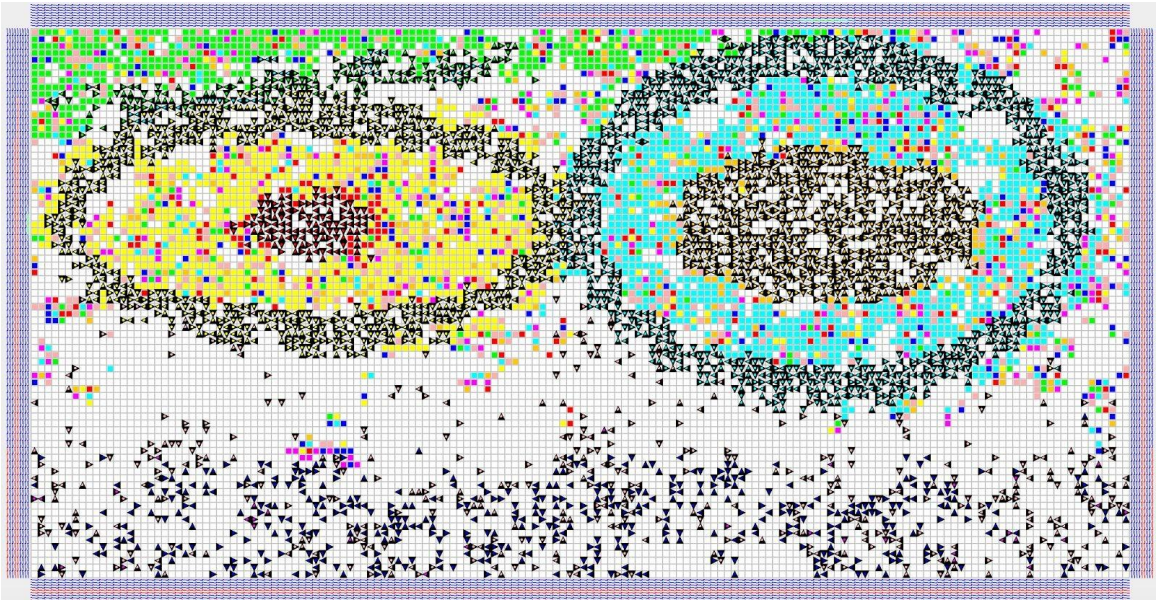

Figure 10: Agent 8 eats agents 1 and 2, representing the degradation of the cellular membrane from ROS reactions

Discussion

The experimental results have been separated into two categories: a quantitative analytical approach, as well as visual representations.

Agent 8 as a Function of Agent 6 & 7 Mating Probability

The quantitative analytical approach for the first segment of the experiment showcases the relationship between the population of agent 8 as a function of the mating parameter probability between agents 6 and 7. The final result was a quartic function. This is representative of iron and PAH coming together in the interstitial space to form ROS. Although the mating parameter does not have a direct correlation to the chemistry regarding the catalytic cycle, it is possible to think of the mating parameter as reactivity. Initially, as the reactivity of the PM present in the lungs increases, the production of ROS increases. However, this population does not increase monotonically; the quartic function has local minima and maxima. The increase in population of agent 8 interferes with further production of agent 8. From the chemical viewpoint,

this can be explained by the fact that as more ROS are formed, they are able to react with themselves or other ROS, and actually terminate the catalytic cycle. For example, if two hydroxyl radicals (OH) come together, they are able to form hydrogen peroxide, which is not a radical species. Moreover, hydrogen peroxide is much less prone to attack cellular structures. Hydrogen peroxide is able to exist over a larger time and with higher concentrations orders of magnitude greater than the hydroxyl radical[18].

Visually for the first segment of the experiments, an increase in the mating parameter probability, results in an increase in the population of agent 8. Also, the visual representation helps further support the conclusion that the sheer population of agent 8 prevents agents 6 and 7 from meeting and mating.

The research regarding kinetics and mechanisms of the catalytic cycle have been studied only in a limited fashion, and generally outside of the human body[14,18]. Results from one study concluded that due to the complexity of the production of ROS within the body, the only statement that is truly valid is that the production of ROS through these catalytic cycles and Fenton type reactions is non linear[18]. Figure 11 shows the results from this study.

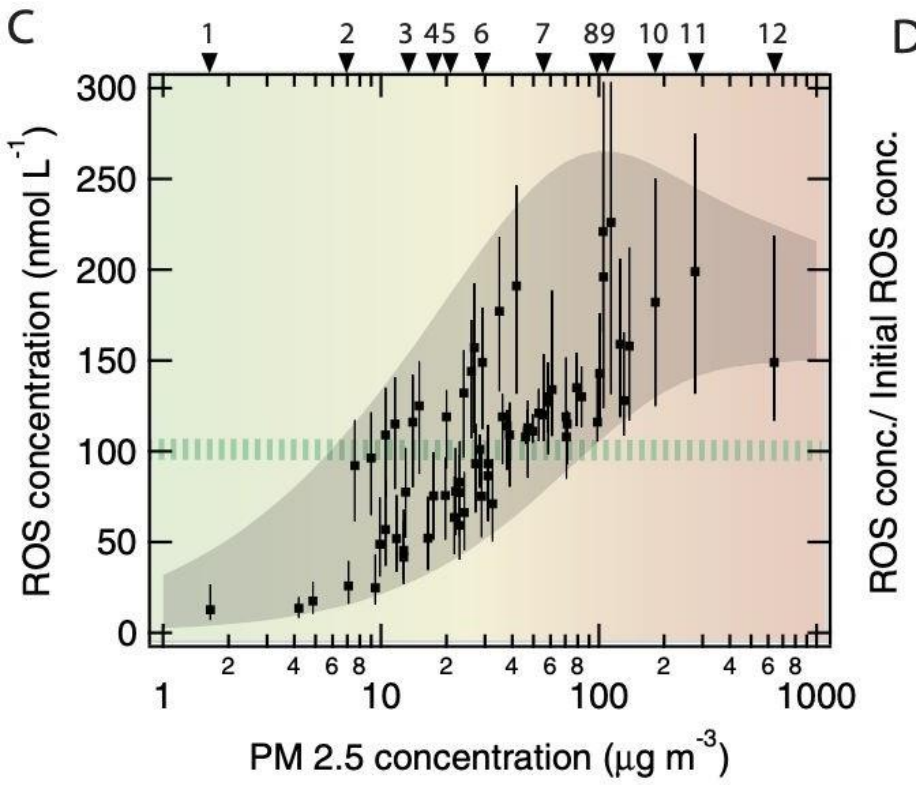

Figure 11: Courtesy of Lake et al. As $PM_{2.5}$ concentrations increase, ROS concentration increases, nonlinearly

Although these results use concentration instead of reactivity, they represent similar findings in the production of ROS within this model, with both containing nonlinear relationships.

Change in Agent 1 and 2 Population as a Function of Agent 8 Population

For the second segment of the experiment, the analytical data is not quite as clear. The change in the populations of agents 1 and 2 is stochastic with the increase in agent 8. Rather than seeing a relationship or function that shows that as agent 8 increases, the change in agents 1 and/or 2 increases with it, the graphs show that there is almost no relationship at all, but a randomness to the loss of agents 1 and 2. Although there is no function representing this relationship, it does seem as though there is an attractor towards the right, lower side of the

figure 6 plot for the change in agent 1. This may be representative of COBWEB, as it pulls the population of agent 8 towards 250-350, with a change of approximately 30 in the population of agent 1. However, this pattern is not reproduced with agent 2 or the total change in the populations of agents 1 and 2. Therefore, it is most likely that there is a randomness to the process of agent 8 eating agents 1 and 2.

In relation to the study of PM, if there were no other evidence besides these stochastic relations, then it would be presumptive to assume that the amount of ROS within the alveolar lung tissue is not correlated to the destruction of the cell or cell apoptosis. This is not consistent with the literature on PM, as it has been widely accepted within the scientific community that as the amount of PM increases within the lungs, the production of ROS increases, which leads to a wide variety of health effects, including cell apoptosis within lung tissue[2-14, 16-18].

The visual results did show a correlation between agent 8 population and the change in the population of agents 1 and 2, but this change was not as prominent as expected. This correlates to the plotted data found in figures 6 through 8. As agent 8 was moved towards the cells, the population of agents 1 and 2 decreased. Figures 9 and 10 show this trend, however, visually, it is uneven. Some parts of the cell membrane, represented by agents 1 and 2 are filled, while others are visually reduced.

Visually, in watching the evolution of the model, it can also be shown that agents 1 and 2 at the bottom part of the cellular membrane are most affected by agent 8, representing ROS. However, when calculating the populations of agents 1 and 2, the total population of the cellular membrane is included.

Moreover, while watching the evolution of the model (videos not included in this report), it was apparent that the change in the population of agents 1 and 2 plateaued. After each experiment, the cellular membrane ended up looking like figure 10. Agent 8 moved into the cellular space, where it initially had an effect on the removal of agents 1 and 2, but as the model progressed, there was no further significant change after this period. This plateau occurred with a population of agent 8 above 200. Below 200 however, the change in the populations of agent 1 and 2 did not reach this same plateau visually; it seemed as though the cellular membranes were still relatively intact. This is an indication again that COBWEB is operating with attractors, pulling the change of population of agents 1 and 2 towards a certain value.

However, this may be subject to the experiments run. The model is looking at varying doses of iron and PAH over a certain time period. If the model was looking at multiple doses, or waves of agent 8, the cellular structure might have deteriorated further. This does explain however the plateau seen visually in the cellular membrane. If there was a continuous stream of agent 8 attacking the cell structures, it might be seen visually that the cellular structures start to fail, and may even have an impact on the empirical data.

The introduction of the immune response has not been implemented into this model. It is important to note that within actual human alveolar tissue, multiple proteins, cytokines, macrophages, and other cellular and physical processes are being completed to remove and dispose of PM, ROS, and other foreign particles, like viruses.

In comparison to literature values, no studies are actually able to determine how many cells die *in vivo* due to PM and ROS. *In vivo* and even *in vitro* studies are only able to account for the reaction cells take towards PM and ROS, like the production of cytokines and alveolar

macrophages. This gives COBWEB an interesting look into cellular destruction with the human body. No other studies can give such a visual representation.

To sum up the findings within this report, and to accurately address the research question, it can be stated that the synergistic relationship between iron and PAH is nonlinear in respect to formation of ROS in a single dose. In regards to the relationship between the concentration of ROS and cellular degradation, COBWEB shows that as the amount of ROS increases, the degradation of cells increases, to a certain point, afterwhich the degradation of the cell plateaus. If a continuous stream had been used, the cellular structures may have deteriorated fully. In this model, it can be seen that the cell is able to withstand the ROS formed.

Conclusion

The study of PM is far from over. Although the WHO and other agencies list PM as a significant health risk to the human population, science is still trying to understand the complexities of environmental toxicology, and the effects the anthropocene has on human health[18].

The results within this paper point towards an ability to run and understand complex modelling within human tissue, giving insight into processes that may not have been able to be understood in the lab. The fact that such a complex process like the formation of ROS from iron and PAH within human tissue can be modelled is a feat in itself.

From the use of COBWEB, the production of ROS from PM was nonlinear, predicted by other research. Moreover, the degradation of the cellular membrane from ROS allowed for a look

into the human body that cannot be seen with a microscope. In this way, COBWEB is an extremely valuable tool, and will be used for years to come.

COBWEB, as a complex system modelling tool, will probably never be finished, as further refinements are always possible. In this model, if agent 8 had been able to leave the interstitial space, this could have modelled the continuous attack of ROS due to PM, and given an insight on how lung tissue degrades over a long period of time, and not just over a single dose.

In continuing the idea of exploration and science, this model can be used for a wide variety of applications. For example, besides just looking at the degradation of human epithelial tissue from ROS, the immune response could also be implemented in this model. Alveolar macrophages, cytokines, and the response of the cell could all be included. Even though this model is quite sophisticated, and takes up quite a lot of computing power, more agents could be imputed to monitor the immune response within the cell to foreign particles like PM.

Moreover, SARS-CoV-2, otherwise known as the COVID-19 virus, has had a huge impact on both the world health and economy. As of April 11th, approximately 100,000 people have died, with over a million cases confirmed worldwide[19]. A global recession has also been induced as stay at home orders and self isolation laws come into effect. This is a crisis the human population has not seen in 100 years, and will be studied for years to come.

This model of the epithelial tissue within the lung is applicable to the study of novel coronavirus, as the propagation of the virus ensues through the use of airway epithelial tissue, and it's cellular components[20]. This model could easily be converted into airway epithelial tissue with varying organelles within the cell. SARS-CoV-2 could be represented by another agent

entering the cell, and using these organelles to amplify it's population. Various other ideas could take hold in this model, like the use of hydroxychloroquine as a potential antiviral medication. Another agent could represent medication that infects or eats the SARS-CoV-2 agent. There are a multitude of different applications this model could have in the study of SARS-CoV-2, and hopefully will be put to good use.

Acknowledgements

I would like to thank Professor Bass for supporting me throughout the year, and all of my friends formed within ENV299, including Wilson, Bill, Christian, and Aria. This has been an amazing learning experience, and I am excited to use the skills I have within this course in other research opportunities.

Appendices

Glossary

Alveolar Epithelial Tissue: The connective tissue between pneumocytes, including type I and type II pneumocytes

Alveoli: At the terminus of bronchioles; air sacs that allow for gas exchange with the use of type I pneumocytes

Apoptosis: Cell death

Bronchi: Air passages diverging from the trachea and entering the lungs, branching into bronchioles

Bronchioles: Smaller air passages branching from the bronchi that lead to the alveoli

Broncho-Alveolar Lavage Fluid: Surfactant within the alveolar space and pulmonary tissue

Catalyst: In chemical terms, a catalyst is a species used in a reaction, but is not used up (the concentration is constant at the beginning and end of the reaction) as it is reformed

Coarse Particulate Matter: Particulate matter with a diameter ranging from maximum 10 microns to minimum 2.5 microns

COBWEB: Complexity and Organized Behaviour Within Environmental Bounds

Cytokines: Special proteins that when released interact with cellular membranes as message carriers - generally in regard to immune response and inflammation

Epithelial Lining Fluid: Present within the respiratory tract - other names include Broncho-Alveolar Lavage Fluid

Epithelial Tissue: Connective tissue

Fine Particles: Particulate matter with a diameter less than 2.5 microns

Heavy Metals: Metals included are mercury, thallium, arsenic, cadmium, chromium, and lead - all extremely toxic

Inflammation/Inflammatory Response: An immune response dictated by macrophages and cytokines within cells

Interstitial Space: The space between pneumocytes that contain surfactant; the main deposit of ultra fine particles occur here

Organic Carbon: Chemistry involving carbon - extremely important as this is life's building blocks

Oxidative Stress: The phenomenon of high levels of damaging oxidants within cells that are not balanced by antioxidants

Particulate Matter: A type of primary or secondary pollutant that is in aerosol form. This aerosol can contain solid, liquid, and gas particles that can be a few nanometres across to hundreds of microns

Peribronchial Tissue: Tissue surrounding the bronchus

Pneumocytes: Alveolar epithelial tissue, but specific to include all the lining cells as well

Polycyclic Aromatic Hydrocarbons: PAH are multi membered organic rings that exhibit aromaticity (following Hückel's rule of 4n+2 pi electrons)
Primary Pollutant: A pollutant that has been released directly into the environment and has not been changed
Pulmonary Tissue: Tissue within the lungs and respiratory system
Reactive Oxygen Species: Oxygen species, generally radicals but also peroxides, that interact within cells in a negative manner - can result in the destruction of tissue and cell apoptosis
Secondary Pollutant: A pollutant that has been released into the environment, but has undergone some chemical or physical change
Trace Metals: Metals that would not normally be found in the environment
Tracheobronchial Region: The region in the respiratory system that contains the trachea and bronchial tree
Ultra Fine Particulate Matter: Particulate matter with a diameter less than 0.1 microns

Setup of COBWEB

As stated in the methods section, the most vital part to forming the model is understanding the structural implications behind alveolar epithelial tissue. To fully encompass this, it needs to be understood that there are two types of pneumocytes: type I and type II, with type I being longer and thinner than type II, which is more cuboidal in shape. This is accomplished by setting the width of the model to 160, and the height to 80. Then, to set up the cellular membrane of the type I pneumocyte, the island parameter under the abiotic tab was used. The size was set to 0.5 for both x and y, and the position values to 0.25 and 0.35 for x and y respectively. An inner island was set inside of the larger island, with the same position, but a smaller size of 0.4 and 0.3 for x and y respectively. To force agent 1 into this confined space, the agent abiotic tab was set for the preference value of 1 for the first island, and 0 for the second island, with the step energy representing the agent abiotic factor, with a value of 10000 being the difference factor.

The same methodology was used for the second cellular membrane for the type II pneumocyte. The size of the first island for type II was 0.5 and 0.7, for x and y respectively, while the positions were set to 0.72 and 0.35 for x and y respectively. The second island for the type II membrane was set at the same position, with the size being set to 0.4 and 0.5 for x and y respectively. The set up then followed the type I pneumocyte cell membrane under the agent abiotic tab.

The capillary mesh network was set using the split functionality, where the angle for both splits was 14 degrees, with the first split having a position of 0.02, and the second split having a position of 0.1. Under the agent abiotic tab, the first preference value for the first island was set to 1 and the second preference value for the second island was set to 0. Both the parameters for the capillary mesh were step energy, and set to 1000, for agent 3.

The nuclei were set up in a similar fashion to the cellular membrane, using the island parameter, with the nucleus for the type I pneumocyte set at 0.25 and 0.35 for the positions of x and y respectively, and set the size to 0.15 for both x and y for agent 4. The nucleus for the type II pneumocyte was set to 0.72 and 0.35 for the x and y positions respectively, and the size was set to 0.3 for both x and y for agent 5. The preference values were set to 1 for the islands, the preference difference values to 1000, and the parameters to step energy for both agents. All of the island's hardness, including for the cellular membrane and nucleus, was set to 20 to ensure a defined boundary.

Lastly, the interstitial space was set using the split abiotic factor. The angle was set to 0 and the split position to 0.75. The sides were left as side 1 = 0 and side 2 = 1, which is standard for the split factor. The preference value for agents 6 and 7 was set to 1, the preference difference value to 100, and the parameter to step energy.

Then, the actual formation of ROS can be accounted for. Under the agents tab, within the 2020 version of COBWEB, two different types of agents are able to mate. Agents 6 and 7 were set to mate with each other, and produce only agent 8. The probability of giving birth to agent 8 was then changed for the experiments.

The starting population value for all the agents, except agent 8, were set to 100. The breed energy and asexual pregnancy value for all the agents within the cellular structure (agents 1 through 5) were set to 10. The asexual breed chance for the agents representing the cellular membrane was set to 10, while for the other cellular structures, the chance was set to 1. This ensures that there is always a large amount of agents representing the cellular structures, and can be easily replaced if lost.

Due to the complexity and amount of agents present in this model, it is useful to fill in the areas representing cellular structure (cellular membrane, nuclei, and capillary mesh network) with the agents needed, so as they do not need to reproduce. This allows for a quick set up of the model and enables experiments to be run much faster. This is found under the edit tab, under select agents.

References

(ACS Citation)

(1) Environment and Climate Change Canada. Mandate and Role: Who we are and What we Do. https://www.canada.ca/en/environment-climate-change/corporate/mandate.html (Accessed January 4th 2020)

(2) Environment and Climate Change Canada. Air Pollution: Particulate Matter 2.5 and 10. https://www.canada.ca/en/environment-climate-change/services/air-pollution/pollutants/common-contaminants/particulate-matter.html (Accessed January 4th, 2020)

(3) Baird, C.; Cann, M. *Environmental Chemistry, 5th Edition.* W H Freeman: New York, **2012**; 118.

(4) Zhang, R.; Wang, G.; Guo, S.; Zamora, M.; Ying, Q.; Lin, Y.; Wang, W.; Hu, M.; Wang, Y. Formation of Urban Fine Particulate Matter. *Chem. Rev.* **2015,** *115*, 3803.

(5) Mazzei, F.; D'Alessandro, A.; Lucarelli, F.; Nava, S.; Prati, P.; Valli, G.; Vecchi, R. Characterization of Particulate Matter Sources in an Urban Environment. *Sci. Total Environ.* **2008,** *81,* 401.

(6) Schroeder, W. H.; Dobson, M.; Kane, D. M.; Johnson, N. D. Toxic Trace Elements Associate with Airborne Particulate Matter: A Review. *J. Air Waste Manage.* **1987,** *37*, 1267.

(7) Mohankumar, S.; Senthilkumar, P. Particulate Matter Formation and its control methodologies for diesel engine: A comprehensive review. *Renew. Sustain. Energy Rev.* **2017**, *80*, 1227.

(8) Kim, K.; Kabir, E.; Kabir, S. A Review on the Human Health Impact of Airborne Particulate Matter. *Environ. Int.* **2015,** *74*, 136.

(9) Pinkerton, K.; Green, F.; Saiki, C.; Vallyathan, V.; Plopper, C.; Gopal, V.; Hung, D.; Bahne, E.; Lin, S.; Menache, M.; Schenker, M. Distribution of Particulate Matter and Tissue Remodelling in the Human Lung. *Environ. Health Perspect.* **2000**, *108*, 1063.

(10) Thompson, J. Airborne Particulate Matter. *J. Occup. Environ. Med.* **2018**, *60*, 392.

(11) Lyu, Y.; Guo, H.; Cheng, T.; Li, X. Particle Size Distributions of Oxidative Potential of Lung-Deposited Particles: Assessing Contributions from Quinones and Water Soluble Metals. *Environ. Sci. Technol.* **2018**, *52*, 6592.

(12) Bates, J.; Fang, T.; Verma, V.; Zeng, L.; Weber, R.; Tolbert, P.; Abrams, J.; Sarnat, S.; Klein, M.; Mulholland, J.; Rusell, A. Review of Acellular Assays of Ambient Particulate Matter Oxidative Potential: Methods and Relationships with Composition, Sources, and Health Effects. *Environ. Sci. Technol.* **2019**, *53*, 4003.

(13) Yu, H.; Wei, J.; Cheng, Y.; Subedi, K.; Verma, V. Synergistic and Antagonistic Interactions among the Particulate Matter Components in Generating Reactive Oxygen Species Based on the Dithiothreitol Assay. *Environ. Sci. Technol.* **2018**, *52*, 2261.

(14) Pardo, M.; Shafer, M.; Rudich, A.; Schauer, J.; Rudich, Y. Single Exposure to near Roadway Particulate Matter Leads to Confined Inflammatory and Defence Responses: Possible Role of Metals. *Environ. Sci. Technol.* **2015**, *49*, 8777.

(15) Weller, M.; Rourke, J.; Overton, T.; Armstrong, F. *Inorganic Chemistry, 7th Edition.* Oxford University Press: New York, 2018; 405.

(16) Meyrick, B.; Reid, L. The Alveolar Wall. *Brit. F. Dis. Chest.* **1970,** *64*, 121.

(17) Brody, J.; Williams, M. Pulmonary Alveolar Epithelial Cell Differentiation. *Annu. Rev. Physiol.* **1992,** *54*, 351.

(18) Lake S. J. P; Berkemeier, T. Tong, H.; Arangio, M. A.; Lucas, K.; Pöschl, U.; Shiraiwa, M. Chemical Exposure-Response Relationship between Air Pollutants and Reactive Oxygen Species in the Human Respiratory Tract. *Sci. Rep.* **2016**, *1*, 1

(19) John Hopkins University. COVID-19 Dashboard by the Center for Systems Science and Engineering at John Hopkins University. https://coronavirus.jhu.edu/map.html (Accessed April 2020)

(20) Matsuyamaa, S.; Naoa, N.; Shiratoa, K.; Kawasea, M.; Saitbo, S.; Takayamab, I.; Nagatac, N.; Sekizukad, T.; Katoha, H.; Katoa, F.; Sakataa, M.; Taharaa, M.; Kutsunae, S.; Ohmagarie, N.; Kurodad, M.; Suzukic, T.; Kageyamab, T.; Takedaa, M. Enhanced isolation of SARS-CoV-2 by TMPRSS2- expressing cells. *Proc. Natl. Acad. Sci. U.S.A.* **2020,** 117, 7001.